Applied Materials Today xxx (xxxx) xxx

Contents lists available at ScienceDirect

Applied Materials Today

journal homepage: www.elsevier.com/locate/apmt

Piezoactive dense diphenylalanine thin films via solid-phase crystallization

Konstantin Romanyuk[a,b,1], Vladislav Slabov[a,1], Denis Alikin[b], Pavel Zelenovskiy[b,c], Maria Rosario P. Correia[d], Kirill Keller[e], Rute A.S. Ferreira[a], Semen Vasilev[f], Svitlana Kopyl[a], Andrei Kholkin[a,b,g,*]

[a] Department of Physics & CICECO–Aveiro Institute of Materials, University of Aveiro, Aveiro, 3810-193 Portugal
[b] School of Natural Sciences and Mathematics, Ural Federal University, 620000, Ekaterinburg, Russia
[c] Department of Chemistry & CICECO–Aveiro Institute of Materials, University of Aveiro, Aveiro, 3810-193 Portugal
[d] Department of Physics & I3N, University of Aveiro, Aveiro, 3810-193 Portugal
[e] Laboratory of Solution Chemistry of Advanced Materials and Technologies, ITMO University, St. Petersburg 197101, Russian Federation
[f] Department of Chemical Science, Bernal Institute, University of Limerick, V94 T9PX Limerick, Ireland
[g] Piezo- and Magnetoelectric Materials Research & Development Centre, Research School of Chemistry & Applied Biomedical Sciences, National Research Tomsk Polytechnic University, Tomsk, Russia

ARTICLE INFO

Article history:
Received 15 August 2021
Revised 29 October 2021
Accepted 3 November 2021
Available online xxx

Keywords:
Piezoelectrics
Thin films
Diphenylalanine
Solid-state crystallization

ABSTRACT

Piezoactive biomaterials are currently in the forefront of the worldwide research due to the multitude of applications ranging from implantable biosensors to biocompatible energy harvesters. Among them, biomolecular piezoelectrics based on amino acids and dipeptides (as exemplified by diphenylalanine, FF) are the most studied. Major problem is an inability to control the self-assembly process to produce dense films with controlled orientation and thickness. To overcome this, we propose a novel method of the formation of crystalline piezoactive FF films via solid phase crystallization directly from the amorphous phase. The process starts from the spin-coating of FF monomers in an organic solution. These layers are then exposed to a controlled humidity that triggers nucleation and growth of highly oriented piezoactive areas (domains). The crystallization process proceeds without changing the morphology and results in dense films with controlled thickness. Large ferroelectric-like domains possess uniform piezoresponse of about 30 pm/V with the in-plane polarization. The growth kinetics is controlled by the temperature and humidity, suggesting that fully in-plane oriented films can be obtained. It is hypothetized that the solid-phase crystallization can be applied to other bioorganic piezoelectrics and thus open an avenue for further use of these materials in implantable piezotronics and beyond.

Piezoelectric materials are widely used in a variety of different applications ranging from microelectromechanical systems (MEMS) to sonars for submarine detection [1]. Recently, the focus of the worldwide research has shifted to biocompatible, implantable and easily recyclable piezomaterials that are prerequisite for the development of wearable, implantable, and digestable microdevices that could serve to both generate charges upon mechanical load or to deform in response to applied voltage. Both effects are becoming increasingly important in biomedicine, e.g. for neurostimulation [2], tissue regeneration [3] or electrical energy harvesting to power implantable devices [4]. During the last decade it has been found that some amino acids [5] and self-assembled dipeptides [6] are suitable biomaterials with high piezoelectric activity and considerable pyroelectric response. In dipeptides, these effects were assigned to anisotropic non-covalent bonding between monomers and appearance of trapped water molecules during self-assembly process [6–9]. This process, trigerred by the water presence, is poorly controlled and results in most cases in randomly oriented nano- and microtubes with unusually high pyro- and piezoresponses. [10,11] These tubes are difficult to use in the aforementioned devices due to the problems with handling and patterning using common microelectronic processes [12]. Several methods have been applied to fabricate thin fims of short dipeptides [13,14] or, at least, to orient their assemblies via substrate treatment [15] or using gravitational force during dip-coating [16]. However, thus obtained assemblies were still poorly adapted for the use in device applications due to high inhomogeneity, apparent porosity, and loose structure.

* Corresponding author.
E-mail address: kholkin@ua.pt (A. Kholkin).
[1] Equal contributions

https://doi.org/10.1016/j.apmt.2021.101261
2352-9407/

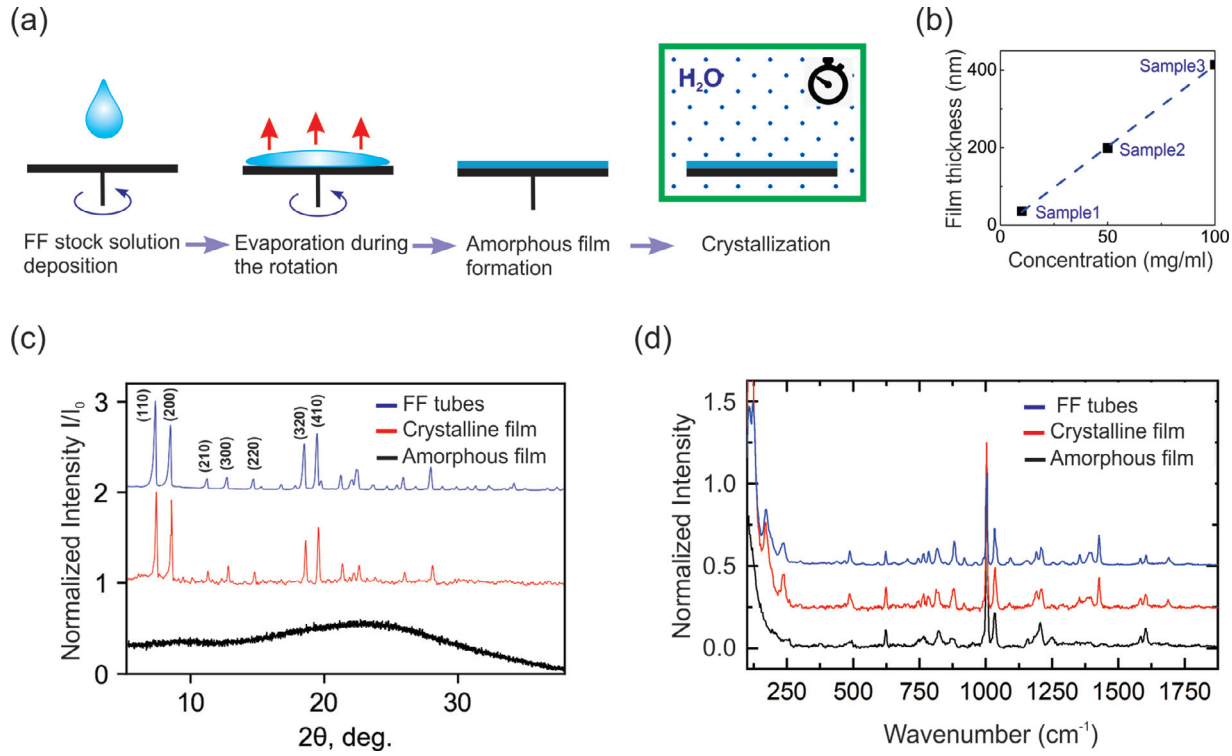

Fig. 1. Preparation and structural characterization of FF films. (a) Schematic of FF film preparation; (b) film thickness as a function of FF concentration in HFIP. PFM, XRD, Raman measurements are shown for the film with the thickness of about 400 nm (Sample 3); (c) XRD and (d) Raman spectra of the film before and after water-vapor treatment. In (d) the peaks in high-frequency range correspond to the vibrations of FF functional groups and they are identical to those observed in the spectra of FF molecules, and the low-frequency part (below 250 cm^{-1}) relates to crystal lattice vibrations.

It is well known that the direct crystallization from the amorphous phase can be used for the development of novel materials and structures. [17,18] Crystallization can be described as the formation of a solid crystalline phase from an amorphous state, leading to a crystalline material, in which growing crystals are embedded in the amorphous matrix [19]. Amorphous phase exists in a metastable state and the crystallization of amorphous materials needs an activation energy, which may be supplied by the thermal or/and mechanical energies. Standard crystallization of FF structures as demonstrated in a number of papers [20,21] is due to a self-assembly of molecular building blocks in a solution that includes the nucleation process and proceeds by Ostwald's step rule through which a coalescence of monomers leads to the formation of nanospheres, which then undergo ripening and structural conversions to form final supramolecular assemblies [20]. A rich diversity of supramolecular polymer nano- and microstructures includes tubes, fibres, films, plates and vesicles. [13,18] These supramolecular materials emerge through the self-assembly of monomeric building blocks, bound together in organized structures by non-covalent interactions [22].

In our work, we present a novel mechanism of the formation of crystalline piezoactive FF structures via a solid phase crystallization directly from the amorphous phase. In contrast to a common process of self-assembly from FF solution, [14,20] proposed mechanism does not require a mass transport and long-range diffusion of FF building blocks being rather a disorder-order phase transition. The transition starts at a certain humidity level and is followed by the nucleation and growth of piezoactive crystalline domains in initially amorphous matrix without notable changes in the morphology and film's thickness. Thus, it is principally different from the self-assembly processes described above.

The preparation procedure of crystalline FF films was divided into two major steps (Fig. 1(a)): (i) fabrication of the amorphous FF films from the hexafluoroisopropanol (HFIP) stock solution by spin-coating method, and (ii) controlled crystallization of the amorphous films in a climatic chamber at a certain level of relative humidity (RH). See the details of the preparation procedure in the Supporting Information section. FF stock solution was prepared by dissolving commerical FF powder in HFIP with the concentration ranging from 1 to 100 mg/mL. To avoid the formation of any kind of aggregates, FF solution was prepared immediately prior to use. To prepare usable amorphous films, it was important to minimize the influence of the atmospheric water during drying and spin-coating procedures. Low surface tension of the HFIP (16 mN/m) [23] allowed good wetting of the used substrates (Pt/SiO_2) and led to their perfect coverage. Similar results were obtained with ITO-coated glass and polymer (PET) substrates.

The drying/spin-coating processing (at 5000 rpm during 30 s) was done under the RH below 50% and fast enough to avoid crystallization during drying. After drying, the obtained films remained stable in the amorphous state and under ambient conditions at the humidity level below 60%. The thicknesses of the obtained amorphous FF films was measued by the optical ellipsometry (Fig. S1). The obtained thin amorphous FF films had thickness depending on the solution concentration and ranging from tens to hundreds nanometers (Fig. 1(b)). The films were further examined with XRD and Raman spectroscopy (Fig. 1 (c, d)). Only a broad halo was observed in XRD diffractograms before an exposure to a humid atmosphere (Fig. 1(c)), thus confirming the amorphous state of the deposited films. The Raman spectroscopy (Fig. 1(d)) also did not reveal any peaks in the low-frequency part (below 400 cm^{-1}) characteristic of the crystal lattice vibrations [24].

The process of the crystallization was further continued in a climatic chamber at high enough humidity. Instability of the amorphous phase of FF film is revealed in the presence of water vapor, and during an exposure to a humid atmosphere (RH 60–90%),

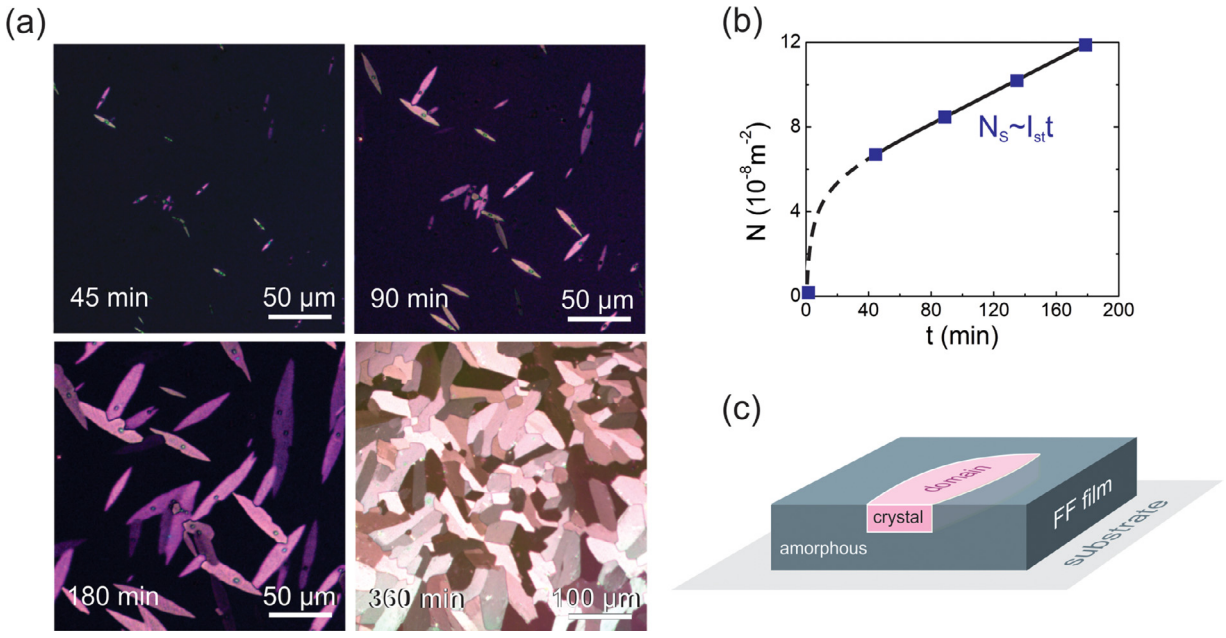

Fig. 2. The growth kinetics of lenticular crystalline domains and variation of domain density with time. (a) Polarized optical microscopy images after sequential exposure of the amorphous FF film to the humid atmospere: domain size increases linearly with the exposure time. (b) 2D density of crystalline domains, N, vs. time. (c) Schematic of the cross-section of the crystalline domain in an amorphous FF film.

the film spontaneously transformed into a more stable crystalline phase. Speed of crystallization is controlled by the temperature and humidity and, at the humidity below 60%, the crystallization process is stopped. It means that the crystallization is directly related to the effect of water molecules on the amorphous phase of the film. At the relative humidity 90% and temperature 30 °C the crystallization is completed within 6 h. The subsequent stages of the domains growth and resulting polycrystalline mosaic structure of the film are shown in the polarized optical microscopy images in Fig. 2.

After exposure to the climatic chamber the films were further examined by the XRD and Raman scattering (Fig. 1 (c, d)). Peaks identical to that of FF microtubes appeared in XRD diffractograms and Raman spectra (Fig. 1 (c, d)) indicating a structural transition from the amorphous to the crystalline phase occurring in the film. The appearance of the crystalline phase was also confirmed by Piezoresponse Force Microscopy (PFM) and optical measurements, as it will be discussed below. The peak positions in XRD and Raman spectra of FF films and FF microtubes were almost coincident, thus allowing us to conclude that the crystalline films possess a typical hexagonal crystal structure with $P6_1$ symmetry characteristic of FF self-assembled nanotubes [25].

The crystallization process of the amorphous FF involves two steps: a nucleation stage and crystal growth stage. The nucleation of crystalline domains occurs mainly at the film surface, after the nucleation domains increase their size linearly with time and at the end of the growth stage the crystalline domains coalescence and form a crystalline film. The kinetics of the nucleation process and schematics of crystalline domain embedded in the amorphous film are shown in Figs. 2(b), and 2 (c), respectively. The kinetics of the nucleation process (Fig. 2(a)) can be described in terms of the classical nucleation theory adopted for the case of heterogeneous nucleation [19]. Heterogeneous nucleation is, in general, a more common phenomenon as compared to the homogeneous one. Specific sites such as surfaces, inclusions, impurities, and defects can trigger the nucleation process. For example, a notable density difference between the amorphous and crystalline phases of FF can be accompanied by a strong surface nucleation. As was observed in the topography images (Figure (3 (a,d)), the elevated height of the crystalline domains implies appreciably lower density for the crystalline phase in comparison with the amorphous one. Therefore, the surface nucleation in FF films should be a dominating process in the crystallization process. The rate of the surface nucleation can be evaluated from the 2D domain density dependence, N, on time in Fig. 2(b). In the beginning (first minutes, Fig. 2(b)), we observed a maximal rate of nucleation occurring at the surface inclusions, impurities and other surface defects. After depletion of the nucleation centers, the rate of the nucleation is reduced (Fig. 2(b)) and the surface nucleation can be described within the framework of classical nucleation theory as a linear dependence of the domains density vs. time: $N_S(t) \propto I_{st}t$, where I_{st} is the steady state nucleation rate and t is the time [19].

In the crystal growth stage, we observed lenticular domains elongated along the fastest growth direction. The observed shape proportions were kept until domain coalescence. The linear dependence of the domain size with time (Fig. 2(a)) implies that major rate-limiting process of crystal growth is the interface reaction mechanism which describes the probability of the attachment of a structural unit (FF molecular) to the crystalline surface. Visualization of the crystalline film's cross-section with scanning electron microscopy does not show any topological features such as microrods, microtubes or others, like those observed in other studies [13,14,26] (Fig. S3). Moreover, detailed analysis of the surface topography (Fig. S3 (b, c)) does not reveal any difference between the amorphous and crystalline regions on both micro- and nano scales. It also indicates that the crystallization process is followed with the minimal displacements and rotations of FF molecules at the amorphous/crystalline interface needed to form an ordered crystalline structure.

Short-range displacements and rotations of FF monomers within their own surroundings in the amorphous phase apparently need significantly lower activation energy and shorter time than the mass transport or long-range diffusion processes and therefore occur primarily. As a result, the initial morphology of the film during the solid phase crystallization remains unchanged in contrast to the standard self-assembly in a solution or solid phase self-

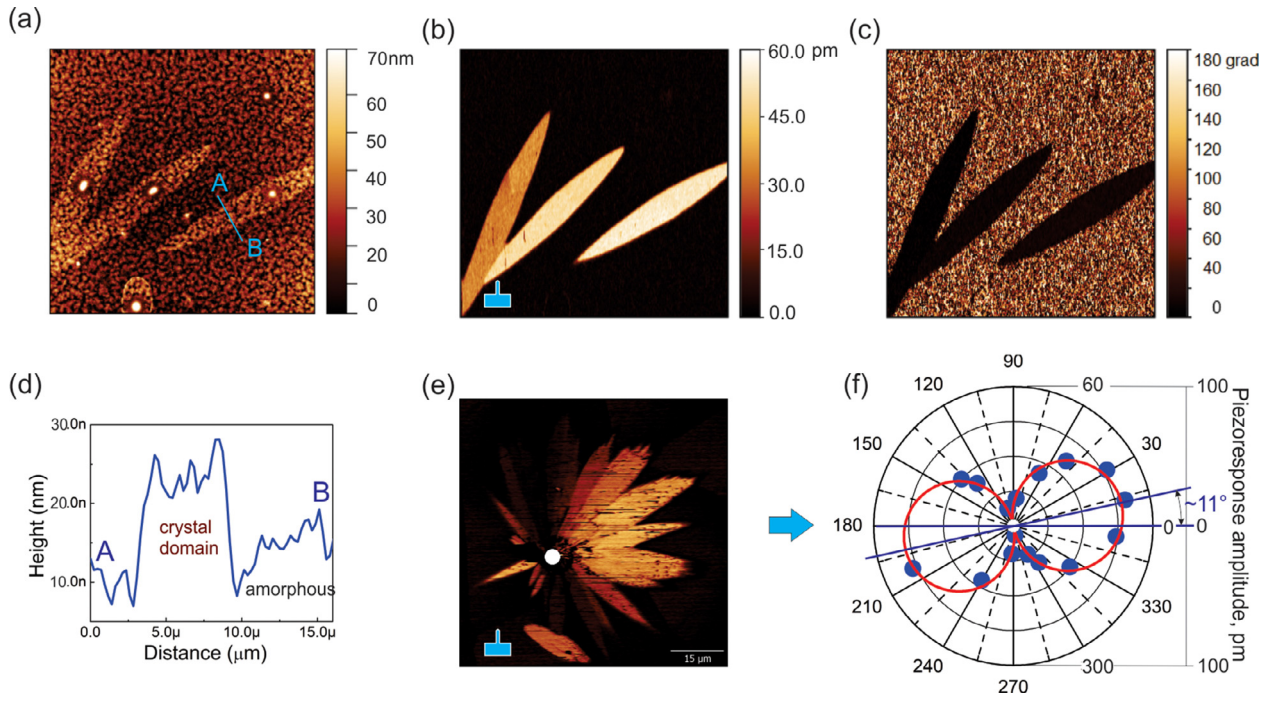

Fig. 3. Topography and PFM imaging of crystalline FF domains. (a) AFM topography of FF film with crystalline domains. (b) Amplitude and (c) phase LPFM images of the crystalline domains. (d) Height profile across crystalline domain phase. (e) LPFM image of the "star-like" crystalline domains structure radially distributed around nucleation point marked by white spot. (f) Angular dependence of LPFM amplitude (red line) for the lenticular crystalline domains in polar coordinates with the zero of the coordinate system located in the nucleation point. Image size is 60 × 60 μm^2.

assembling process, [14,20,26] which are characterized by the significant mass transport of the material and morphological changes resulting in the equilibrium crystalline shapes such as micro/nanotubes and others.

The particularity of the obtained polycrystalline films is an arbitrary in-plane orientation of the polarization of the crystalline domains, so the orientation of crystallographic directions relative to the normal of the film's plane is the same for all domains. It is confirmed by the identical shape of growing 2D domains (before their coalescence) and very close piezoresponse amplitudes. We suggest that the observed crystallographic orientation within domains is defined by the surface nucleation process, i.e. it is the film's surface that serves as an orienting factor at the moment of the nucleation of the crystalline phase. We beleive that, at the RH of 80 – 90%, water condensation does not occur and, therefore, no dissolution of the amorphous FF film happens. However, the concentration of the water vapor at the film's surface is high enough to initiate the solid phase crystallization process which results in the drastic change of functional properties in the growing domains. In contrast to amorphous background, the crystalline regions rotate vector of polarized light (Figure S2) and exhibit a clear PFM contrast (Fig. 3 (b,c,e)).

Piezoelectric properties of the films were studied by vector PFM in both lateral (LPFM) and vertical (VPFM) signals. Angle-dependent LPFM with piezoresponse amplitude distribution for crystalline FF film is shown in Fig. S4.2 and Fig. 3(f). In LPFM mode all domains exhibit close values of PFM amplitude up to 30 pmV^{-1} with polarization vector oriented along the fastest growth direction (Fig. 3(e-f)). (In Fig. 3(f) the polarization vector slightly deviates from the fastest growth direction by ~11°). The defined polarization vector orientation is in agreement with the optical contrast data for a crystalline domain in polarized light at different rotational angles (Fig. S2), so, based on the optical contrast dependence, we conclude that the polar axis of the FF crystal should be along the fastest growth direction of the crystalline domain. To identify the crystal structure of the domains, orientation of crystallographic directions in the domains, and components of the measured piezo tensor, we performed a detailed analysis of XRD and Raman data. We argue that the molecular structure of crystalline domains of the film is very similar to that of FF micro/nano tubes (Fig. 4), so that the main symmetry axis C_6 and polarization vector are both lying in the plane of the film. This also agrees well with the values of the in-plane piezoresponse coefficient d_{15}, which are close to the values reported previously on peptide micro/nanotubes (diameter ~100 nm) [6].

In order to determine the orientation of the nanotubular crystal structure in the crystalline domains, polarized Raman mapping was performed in the "star-like" arrays of the domains with joint center (Fig. 4(a)). This structure allows obtaining several polarization geometries in one Raman map. The direction of the laser polarization was parallel to the analyzer and oriented horizontally (yellow and blue arrows in Fig. 4(a)).

The Raman map presented in Fig. 4(a) corresponds to the spatial distribution of the intensity of the spectral line located around 120 cm^{-1} and demonstrates the crystallinity of the domains in contrast to the amorphous layer around [24] . Angles between the domains axes and laser polarization are also presented in Fig. 4(a). The middle frequency region of Raman spectra measured within the domain is shown in Fig. 4(b). This region contains lines corresponding to the vibrations of various functional groups of FF molecule [24]. The most important lines here are located at 487 cm^{-1} (NH_3 group torsion vibrations), 1003 cm^{-1} (in-plane breathing vibrations of phenyl rings), 1251 cm^{-1} (amide III line – combination of N-–H in-plane-bending and C–N stretching vibrations), 1467 cm^{-1} (symmetric stretching vibrations of COO^-), and 1689 cm^{-1} (amide I line – mainly associated with the C=O stretching vibrations) [24,27,28]. To determine the spatial orientation of the nanotubular crystal structure in the domains the intensities of abovementioned lines were analyzed.

Raman spectra show that intensities of the Amide I line and the line corresponding to COO– group are stronger at low angles and became weak at higher angles. This means that C=O and

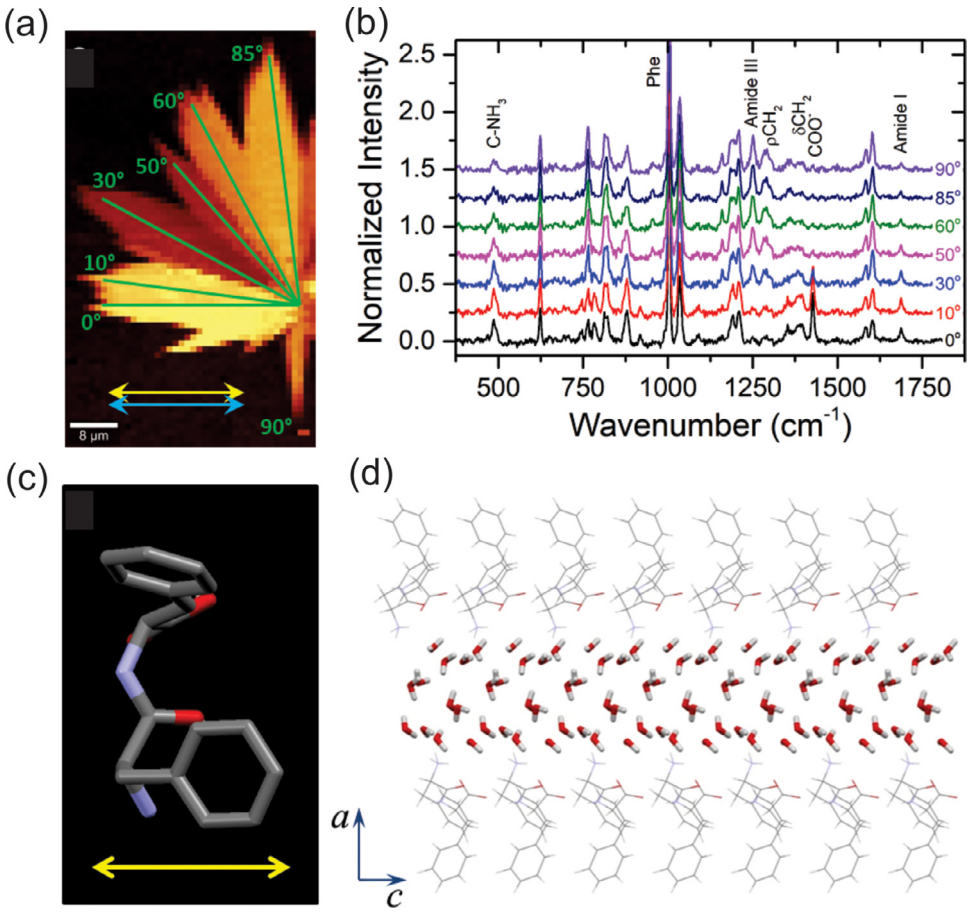

Fig. 4. Angular-resolved Raman spectroscopy of the lenticular crystalline domains. (a) Raman map constructed by the intensity of spectral line at around 120 cm^{-1}. (b) Raman spectra measured in lenticular crystalline domains with the different orientation relative to laser polarization. (c) Suggested orientation of the FF molecule in the horizontal domains relative to the laser light polarization. (d) Suggested orientation of the $P6_1$ crystal in the horizontal domains relative to the laser polarization. The direction of the laser polarization was parallel to the analyzer and was oriented horizontally (yellow and blue arrows in (a)).

COO– groups are mainly oriented horizontally, i.e. along the direction of laser polarization. At the same time, Amide III line is very strong at higher angles with maximum intensity at 90° thus showing that C-–N bonds are oriented vertically relative to the laser polarization. The intensity of NH_3 torsional vibrations weakly depends on the angle. Therefore, the axis of this vibration should mostly coincide with the laser beam propagation. The most intensive line at 1003 cm^{-1} corresponding to breathing vibrations of phenyl rings has a maximum at about 60° thus allowing to suggest that the planes of the rings are oriented at 60° to the direction of laser polarization. All these observations allowed us to suggest the most probable orientation of FF molecules in the crystalline domains (Fig. 4(c)). Such molecule orientation is characteristic of FF micro/nanotubes oriented by its c-axis mostly along the polar (0°) direction of the domains (Fig. 4(d)). This fact is compatible with the preferential growth direction along the polar direction. Temperature stability of the grown films was confirmed by the temperature-dependent Raman scattering (Fig. S5.1). It follows that the structural changes in FF films occur at the temperature 120° (very similar to self-assembled FF micro/nanotubes) suggesting that the variations of the piezoelectric properties with temperature should be similar to those reported in Ref. 7,11 and 29.

Since the piezoelectric reponse of the FF films is inherited from the piezoelectric properties of the individual nanotubes, we hypothetize that FF films possess not only shear (d_{15}), but also transverse $d_{31} = d_{32}$ and longitudinal d_{33} piezocoefficients (d_{33} = 17.9 pm/V, [6]) which make them a versatile piezoelectric material for different applications. The choice of the possible structure for sensor or actuator element depends on the configuration of the film and electrodes, as well as on the mode of its excitation. If the shear piezoelectric coefficient is used (provided the grown domain is sufficiently large) the cantilever or membrane structure can be made as shown in Figs. S6.1 and S6.2. Surface acoustic waves (SAW) can be detected based on high shear piezoelectric coefficients piezoelectric laminates [30]. Because of their fully biocomaptible and biodegradable nature, FF film sensors/harvesters (or actuators) can be used in transient implantable electromechanical devices as recently demonstrated in glycine-PVA films in [31].

In conclusion, a novel mechanism of the formation of piezoactive crystalline FF structures via solid phase crystallization from the amorphous FF phase is presented. The approach is validated by the formation of the piezoactive FF films via a two-stage process: first, spin-coating of the amorphous films and then their crystallization under the action of water-vapor treatment in a climatic chamber. The demonstrated mechanism is well reproducible, simple in realization, and promising for practical applications. The structure and orientation of the crystalline films were identified with X-ray diffraction and angle-dependent Raman spectroscopy. Both are compatible with the structure of FF micro/nano tubes of the symmetry C_6 with the symmetry axis and polarization vector lying in the plane of the film. The obtained crystalline films demonstrate strong lateral piezoresponse of about 30 pm/V within the domains and thus can be used as templates for further patterning and device fabrication. We believe that implementation of the solid phase

crystallization method validated for model diphenylalanine can be used for the synthesis of other biomolecular materials prone to crystallization in the water vapor atmosphere. With their natural biocompatibility, flexibility, and reproducibility combined with strong piezoelectricity such films can find multiple applications in implantable and wearable electronics.

Declaration of Competing Interest

The authors declare that they have no known competing financial interests or personal relationships that could have appeared to influence the work reported in this paper

CRediT authorship contribution statement

Konstantin Romanyuk: Investigation, Data curation, Visualization, Writing – original draft. **Vladislav Slabov:** Data curation, Investigation, Writing – original draft. **Denis Alikin:** Methodology, Investigation, Data curation, Writing – original draft. **Pavel Zelenovskiy:** Methodology, Investigation, Data curation, Visualization, Writing – original draft. **Maria Rosario P. Correia:** Data curation, Writing – review & editing. **Kirill Keller:** Investigation. **Rute A.S. Ferreira:** Data curation, Writing – review & editing. **Semen Vasilev:** Investigation. **Svitlana Kopyl:** Conceptualization, Investigation, Writing – review & editing, Funding acquisition. **Andrei Kholkin:** Conceptualization, Supervision, Writing – review & editing, Funding acquisition.

Acknowledgments

This work was developed within the scope of the project CICECO-Aveiro Institute of Materials, UIDB/50011/2020 & UIDP/50011/2020, financed by national funds through the FCT/MEC and when appropriate co-financed by FEDER under the PT2020 Partnership Agreement. It is also funded by national funds (OE), through FCT – Fundação para a Ciência e a Tecnologia, I.P., in the scope of the framework contract foreseen in the numbers 4, 5 and 6 of the article 23, of the Decree-Law 57/2016, of August 29, changed by Law 57/2017, of July 19. This work was also suported within the scope of the project i3N, IDB/50025/2020 & UIDP/50025/2020, financed by national funds through the FCT/MEC. P.Z., S.K. and A.K. were partly supported by the FCT (Portugal) through the project “BioPiezo”- PTDC/CTM–CTM/31679/2017 (CENTRO-01–0145-FEDER-031679). The authors thank Dr P. S. Andre for the help with the ellipsometry measurements. Growth of the diphenylalanine films with controllable thickness was done in Ural Federal University. This part of research was made possible by Russian Science Foundation (Grant 19–72–10076). S.V. thanks the financial support by Career-FIT that has received funding from the European Union’s Horizon 2020 research and innovation programme under the Marie Skłodowska-Curie grant (agreement No. 713654). The equipment of the Ural Center for Shared Use “Modern nanotechnology” Ural Federal University (Reg.№ 2968) was used with the financial support of the Ministry of Science and Higher Education of the Russian Federation (Project № 075-15-2021-677).

Supplementary materials

Supplementary material associated with this article can be found, in the online version, at doi:10.1016/j.apmt.2021.101261.

References

[1] K. Uchino, The development of piezoelectric materials and the new perspective, in: K. Uchino (Ed.), Advanced Piezoelectric Materials, Science and Technology, Woodhead Publishing Series in Electronic and Optical Materials, Woodhead Publishing, Sawston, Cambridge, 2010, pp. 1–85, doi:10.1533/9781845699758.1.
[2] C. Rojas, M. Tedesco, P. Massobrio, A. Marino, G. Ciofani, S. Martinoia, R. Raiteri, Acoustic stimulation can induce a selective neural network response mediated by piezoelectric nanoparticles, J. Neural Eng. 15 (2018) 036016, doi:10.1088/1741-2552/aaa140.
[3] A.H. Rajabi, M. Jaffe, T.L. Arinzeh, Piezoelectric materials for tissue regeneration: a review, Acta Biomater. 24 (2015) 12–23, doi:10.1016/j.actbio.2015.07.010.
[4] C. Dagdeviren, B.-.D. Yang, Y. Su, P.L. Tran, P. Joe, E. Anderson, J. Xia, V. Doraiswamy, B. Dehdashti, X. Feng, Bi. Lu, R. Poston, Z. Khalpey, R. Ghaffari, Y. Huang, M.J. Slepian, J.A. Rogers, Conformal piezoelectric energy harvesting and storage from motions of the heart, lung, and diaphragm, Proc. Natl. Acad. Sci. 111 (2014) 1927–1932, doi:10.1073/pnas.1317233111.
[5] S. Guerin, A. Stapleton, D. Chovan, R. Mouras, M. Gleeson, C. McKeown, M.R. Noor, C. Silien, F.M.F. Rhen, A.L. Kholkin, N. Liu, T. Soulimane, S.A.M. Tofail, D. Thompson, Control of piezoelectricity in amino acids by supramolecular packing, Nat. Mater. 17 (2018) 180–186, doi:10.1038/nmat5045.
[6] A.L. Kholkin, N. Amdursky, I. Bdikin, E. Gazit, G. Rosenman, Strong Piezoelectricity in Bioinspired Peptide Nanotubes, ACS Nano 4 (2010) 610–614, doi:10.1021/nn901327v.
[7] P. Zelenovskiy, V. Yuzhakov, A. Nuraeva, M. Kornev, V.Ya. Shur, S. Kopyl, A. Kholkin, S. Vasilev, S.A.M. Tofail, The effect of water molecules on elastic and piezoelectric properties of diphenylalanine microtubes, IEEE Trans. Diel. Electr. Insul. 27 (2020) 1474–1477, doi:10.1109/TDEI.2020.008921.
[8] V. Slabov, S. Kopyl, M. Soares dos Santos, A. Kholkin, Piezoelectricity in self-assembled peptides: a new way towards electricity generation at nanoscale, in: S.J. Kim, A. Chandrasekhar, N.R. Alluri (Eds.), Nanogenerators, IntechOpen, 2019, doi:10.5772/intechopen.89703.
[9] F. Salehli, A.O. Aydin, D. Chovan, S. Kopyl, V. Bystrov, D. Thompson, S.A.M Tofail, A. Kholkin, Nanoconfined water governs polarization-related properties of self-assembled peptide nanotubes, Nano Select 2 (2021) 817–829, doi:10.1002/nano.202000220.
[10] A. Esin, I. Baturin, T. Nikitin, S. Vasilev, F. Salehli, V.Ya. Shur, A.L. Kholkin, Pyroelectric effect and polarization instability in self-assembled diphenylalanine microtubes, Appl. Phys. Lett. 109 (2016) 142902, doi:10.1063/1.4962652.
[11] (a) S. Vasilev, P. Zelenovskiy, D. Vasileva, A. Nuraeva, V. Ya. Shur, A.L. Kholkin, Piezoelectric properties of diphenylalanine microtubes prepared from the solution, J. Phys. Chem. Sol. 93 (2016) 68–72, doi:10.1016/j.jpcs.2016.02.002; (b) A. Nuraeva, S. Vasilev, D. Vasileva, P. Zelenovskiy, D. Chezganov, A. Esin, S. Kopyl, K. Romanyuk, V. Ya. Shur, A.L. Kholkin, Evaporation-driven crystallization of diphenylalanine microtubes for microelectronic applications, Cryst. Growth Des. 16 (2016) 1472–1479, doi:10.1021/acs.cgd.5b01604.
[12] N.B. Sopher, Z.R. Abrams, M. Reches, E. Gazit, Y. Hanein, Integrating peptide nanotubes in micro-fabrication processes, J. Micromech. Microeng. 17 (2007) 2360–2365, doi:10.1088/0960-1317/17/11/025.
[13] (a) N. Hendler, N. Sidelman, M. Reches, E. Gazit, Y. Rosenberg, S. Richter, Formation of well-organized self-assembled films from peptide nanotubes, Adv. Mater 19 (2007) 1485–1488, doi:10.1002/adma.200602265; (b) V. Nguyen, R. Zhu, K. Jenkins, R. Yang, Self-assembly of diphenylalanine peptide with controlled polarization for power generation, Nat Commun 7 (2016) 13566, doi:10.1038/ncomms13566.
[14] J. Ryu, C.B. Park, Solid-phase growth of nanostructures from amorphous peptide thin film: effect of water activity and temperature, Chem. Mat. 20 (2008) 4284–4290, doi:10.1021/cm800015p.
[15] S. Almohammed, S.O. Oladapo, K. Ryan, A.L. Kholkin, J.H. Rice, B.J. Rodriguez, Wettability gradient-induced alignment of peptide nanotubes as templates for biosensing applications, RSC Adv. 6 (2016) 41809, doi:10.1039/C6RA05732B.
[16] J.H. Lee, K. Heo, K. Schulz-Schönhagen, J.H. Lee, M.S. Desai, H.E. Jin, S.W. Lee, Diphenylalanine peptide nanotube energy harvesters, ACS Nano 12 (2018) 8138–8144, doi:10.1021/acsnano.8b03118.
[17] V. Andronis, G. Zografi, Crystal nucleation and growth of indomethacin polymorphs from the amorphous state, J. Non-Cryst. Solid. 271 (2000) 236–248, doi:10.1016/S0022-3093(00)00107-1.
[18] A. Newman, G. Zografi, What we need to know about solid-state isothermal crystallization of organic molecules from the amorphous state below the glass transition temperature, Mol. Pharmaceut. 17 (2020) 1761–1777, doi:10.1021/acs.molpharmaceut.0c00181.
[19] M. Allix, L. Cormier, Crystallization and glass-ceramics, in: J.D. Musgraves, J. Hu, L. Calvez (Eds.), Springer Handbook of Glass, Springer Handbooks, Springer, Cham, 2019, pp. 113–167, doi:10.1007/978-3-319-93728-1_4.
[20] A. Levin, T.O. Mason, L. Adler-Abramovich, A.K. Buell, G. Meisl, C. Galvagnion, Y. Bram, S.A. Stratford, C.M. Dobson, T.P.J. Knowles, E. Gazit, Ostwald’s rule of stages governs structural transitions and morphology of dipeptide supramolecular polymers, Nat. Commun. 5 (2014) 5219, doi:10.1038/ncomms6219.
[21] H. Chen, M. Li, Z. Lu, X. Wang, J. Yang, Z. Wang, F. Zhang, C. Gu, Y.Sun W.Zhang, J. Sun, W. Zhu, X. Guo, Multistep nucleation and growth mechanisms of organic crystals from amorphous solid states, Nat. Commun. 10 (2019) 3872, doi:10.1038/s41467-019-11887-2.
[22] C. Yuan, W. Ji, R. Xing, E. Gazit, X. Yan, Hierarchically oriented organization in supramolecular peptide crystals, Nat. Rev. Chem. 3 (2019) 567, doi:10.1038/s41570-019-0129-8.
[23] I. Colomer, A.E.R. Chamberlain, M.B. Haughey, T.J. Donohoe, Hexafluoroisopropanol as a highly versatile solvent, Nat. Rev. Chem. 1 (2017) 0088, doi:10.1038/s41570-017-0088.

[24] A. Krylov, S. Krylova, S. Kopyl, A. Krylov, F. Salehli, P. Zelenovskiy, A. Vtyurin, A. Kholkin, Raman Spectra of Diphenylalanine Microtubes: polarisation and Temperature Effects, Crystals 10 (2020) 224, doi:10.3390/cryst10030224.
[25] (a) C. Görbitz, Nanotube formation by hydrophobic dipeptides, Chem.-Eur. J. 7 (2001) 5153 doi:10.1002/1521-3765(20011203)7:23⟨5153::AID-CHEM5153⟩3.0.CO;2-N; (b) C. Görbitz, The structure of nanotubes formed by diphenylalanine, the core recognition motif of Alzheimer's β-amyloid polypeptide, Chem. Comm. (2006) 2332, doi:10.1039/B603080G.
[26] J. Ryu, C.B. Park, High-temperature self-assembly of peptides into vertically well-aligned nanowires by aniline vapor, Adv. Mater. 20 (2008) 3754, doi:10.1002/adma.200800364.
[27] B. Hernández, F. Pflüger, S. Kruglik, M. Ghomi, Characteristic Raman lines of phenylalanine analyzed by a multiconformational approach, J. Raman Spectr. 44 (2013) 827–833, doi:10.1002/jrs.4290.
[28] B. Lekprasert, V. Korolkov, A. Falamas, V. Chis, C.J. Roberts, S.J.B. Tendler, I. Notinghe, Investigations of the supramolecular structure of individual diphenylalanine nano- and microtubes by polarized raman microspectroscopy, Biomacromolecules 13 (2012) 2181–2186, doi:10.1021/bm3005929.
[29] A. Heredia, I. Bdikin, S. Kopyl, E. Mishina, S. Semin, A. Sigov, K. German, V. Bystrov, J. Gracio, A.L. Kholkin, Temperature-driven phase transformation in self-assembled diphenylalanine peptide nanotubes, J. Phys. D: Appl. Phys. 43 (2010) 462001, doi:10.1088/0022-3727/43/46/462001.
[30] H. Altammar, N. Salowitz, Ultrasonic structural health monitoring approach to predict delamination in a laminated beam using d_{15} piezoelectric sensors, J. Nondestruct. Eval. Diagn. 4 (2021) 031007, doi:10.1115/1.4050521.
[31] F. Yang, J. Li, Y. Long, Z. Zhang, L. Wang, J. Sui, Y. Dong, Y. Wang, R. Taylor, D. Ni, W. Cai, P. Wang, T. Hacker, X. Wang, Wafer-scale heterostructured piezoelectric bio-organic thin films, Science 373 (2021) 337–342, doi:10.1126/science.abf2155.